Operational Characteristics of a New Energy-saving Impeller for Gas–Liquid Mixing

Serafim D. Vlaev[1*], Paul Mavros[2], Pavel Seichter[3] and Reg Mann[4]

[1] *Institute of Chemical Engineering at the Bulgarian Academy of Sciences, Acad. G. Bonchev Str. Bl. 103, 1113 Sofia, Bulgaria*
[2] *Department of Chemistry, Aristotle University, Thessaloniki, Greece*
[3] *Techmix, Brno, Czech Republic*
[4] *Department of Chemical Engineering, UMIST, Manchester, England*

The fluid dynamic and mixing characteristics of a new hydrofoil impeller (termed Narcissus) for gas–liquid mixing are reported. This impeller provides significant energy-savings in bioreactor applications. Dye-tracer visualization and CFD simulation have been used to uncover the prevailing flow patterns and the impeller liquid flow map is identified. Flow regime boundaries are shifted from those for disc-style turbines. A mixing time corresponding to the turbulent mixing regime (i.e., $Re > 10^4$) is determined. The power characteristics are measured and compared with experimental data obtained for other impellers. The power number for the turbulent mixing regime for both cylindrical and square vessels was as low as 1. The aeration power at moderate Froude numbers (i.e., $Fr < 1$) decreased typically by only between 10 and 30%, confirming good gas-handling capabilities for the new geometry. The gas hold-up at a given power input was greater than for flat-blade disc-style turbines.

Les caractéristiques d'écoulement et de mélange en milieu gaz–liquide d'une nouvelle turbine à pales profilées (appelée Narcissus) sont présentées. Une telle turbine permet une économie d'énergie importante dans les applications de bioréacteurs. On a eu recours à la visualisation par traceurs colorés et à la simulation numérique pour déterminer les profils d'écoulement. La carte d'écoulement de la turbine a été obtenue. Les limites des régimes d'écoulement sont modifiées par rapport à ceux des turbines de type disque. Le temps de mélange correspondant au régime de mélange turbulent (soit $Re > 104$) est déterminé. Les caractéristiques de puissance sont mesurées puis comparées aux données expérimentales obtenues pour d'autres turbines. Le nombre de puissance pour le régime de mélange turbulent pour des réservoirs cylindrique et carré est aussi bas que 1. La puissance d'aération à des nombres de Froude modérés (soit $Fr < 1$) diminue typiquement de seulement 10 à 30 % confirmant ainsi les bonnes caractéristiques de cette nouvelle géométrie pour les milieux aérés. La rétention de gaz à consommation de puissance donnée est plus grande que pour les turbines de type disques à pales verticales.

Keywords: gas–liquid mixing, fluid foil impeller, fluid dynamic characteristics.

The development of mixer agitator designs which provide a measure of control over the balance of fluid mixing and gassing in industrial fluids, by creating balance between shear and flow at low power, presents a continuing challenge. This challenge has been partially met by designing new mixing impellers. The specific flow properties of new designs are characterized by instrumental and numerical techniques (e.g., Mavros, 2001; Bertrand and Xuereb, 1999). Improving mixing performance at low power has been discussed recently by several authors. Fort et al. (1999) reported an axial flow impeller with a high solidity ratio, and Mishra et al. (1998) discussed a wide-blade hydrofoil impeller indicated by APV-B2. An impeller for efficient gassing has also been reported by EKATO (1998).

With reference to our practice (Lossev et al., 1997), pilot experiments using a new impeller termed Narcissus (NS) showed a significant improvement in antibiotic production at low energy input. This finding is important given industry conditions, 100 m^3 bioreactors operating at 1 kW /m^3 for longer than 100 h per batch. For this impeller, energy-savings of more than 30% have been reported by Kraitschev et al. (1999). Nevertheless, no detailed study has yet been published to explain the basis for this improved behaviour.

To classify the NS turbine, a detailed characterization of the unit has been carried out. Studies of the NS impeller have been undertaken separately by Vlaev et al. (2001) and Pesl and Seichter (2000). To further expand available information on hydrofoils, the present paper intends to add detailed fluid dynamic characteristics of this new impeller to their database. Mass transfer and heat transfer characteristics will be published later.

Experimental

The NS turbine is shown schematically in Figure 1a. It contains a supporting disc fitted with an even number of concave, equal-surface blades. Neighbouring blades are positioned on both sides of the disc, symmetrically over and under the supporting disc plane. The blades are positioned to make an acute angle α with the supporting disc plane. The angle and blade shapes can be selected so as to manipulate power consumption and gas dispersion capacity. In this paper, a wide-blade version with a solidity ratio of 0.9 and a blade angle 30°, suitable for transitional mixing, was tested. A 3-D view of the impeller is shown in Figure 1f.

**Author to whom correspondence may be addressed. E-mail address: mixreac@ bas.bg*

Semi-technical scale, flat-bottomed vessels with T = 0.2 m, 0.3 m and 0.4 m with four baffles (0.1T) were used for the experiments. The impeller diameter and clearance were most often $T/3$ and in some cases $T/2$. The vessel was filled with liquid up to level H, equal to the vessel diameter. Given our application objectives, both square and cylindrical vessels were tested. Radial flow impellers such as the Rushton disc-style flat-blade turbine (RT) and the Scaba hollow-blade (Sc) turbines, as well as axial flow impellers such as Lightnin A315, were used for comparison (Figure1b-e). In this paper, only data for A315 with a blade angle of 40° at the hub (denoted as A315/40) are presented. The 45°-inclined-blade turbine and impeller Mixel TT were also used in two separate cases. The scale and the sizes of the components are shown in Table 1.

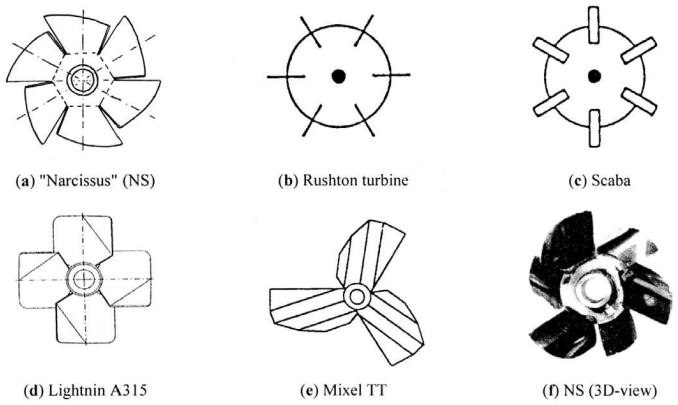

Figure 1. Top views of the novel NS impeller and the reference impellers used in this work.

Table 1. Vessel and agitator characteristics.

Impeller	Diameter, (m)	Vessel size, (m)	D/T	Vessel type
NS	0.13	0.4	0.33	cyl
	0.10	0.3	0.33	cyl
	0.10	0.2	0.50	square
RT	0.13	0.4	0.33	cyl
	0.10	0.20	0.50	square
Sc	0.12	0.4	0.30	cyl
A315	0.12	0.4	0.30	cyl
	0.10	0.2	0.50	square
Mixel TT	0.10	0.2	0.50	square

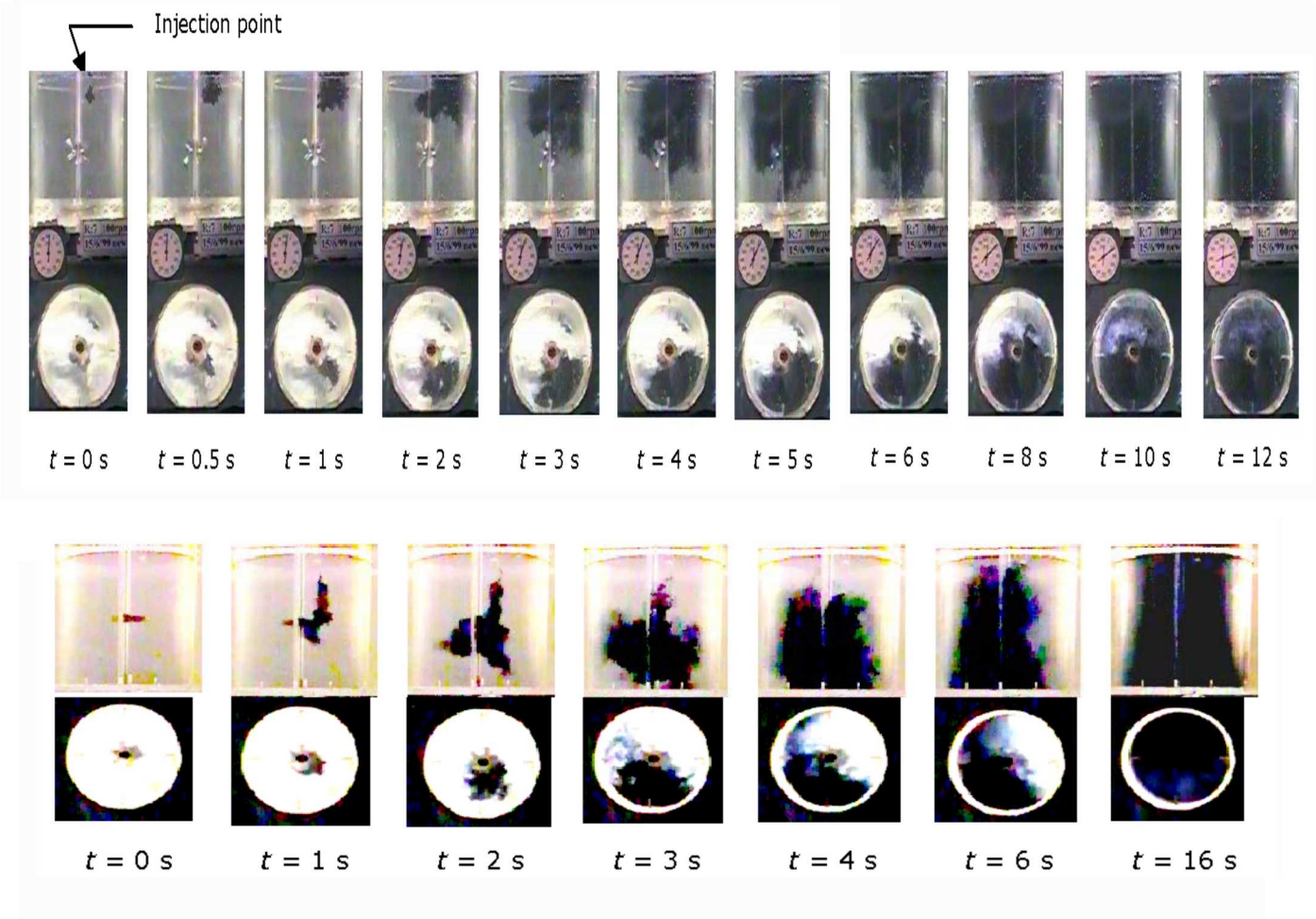

Figure 2. 3-D visualization of mixing by the NS impeller (top) and the 45°- inclined blade turbine (bottom) in a cylindrical vessel, showing the prevailing flow pattern. Tracer: nigrosine, V_L = 23 L, N = 1.6 s^{-1}, D/T = 1/3, C/T = 1/2 (Masoud et al., 1999).

The liquid phase was either water or a water solution of glycerol and 0.5% xanthan gum in water, ensuring viscosity or an apparent viscosity, respectively, of up to 80 mPa·s. In the case of xanthan gum solution, the consistency coefficient was 2.27 Pa·s^n and the flow index was 0.23. Calculation of apparent viscosity via the shear rate was carried out by using the Metzner constant $k_s = 8.1$, and determined separately for NS by following the procedure recommended by Metzner (Chhabra et al., 1999).

Air was used for gassing. Gas flow rates were adjusted to ensure relative flow rates of 0.2 to 1.5 vvm. In all cases, multi-orifice gas spargers, e.g., pipes with holes, were used.

Liquid flow patterns generated by the various impellers were determined via tracer visualization experiments using nigrosine dye. The spread of nigrosine following a dye pulse input was videod (Masoud et al., 1999).

3-D computational fluid dynamics (CFD) simulations paralleled some of the experiments. Commercial CFD code Fluent 5.1 was used, with Gambit 2.1 for meshing. Combined structured and unstructured grids were applied. The number of cells was 120 000. For this work, the sliding mesh technique (Brucato et al., 1998) was employed. Considering the model assessment by Jenne and Reuss (1999), the k-ε turbulence model was adopted. The computer platform included an Intel Pentium III 256 Mb RAM at 450 MHz. CPU time was about 20 h. The details of this study have been reported elsewhere (Staykov et al., 2000).

Gas–liquid mixing regimes were determined by visual observation following the rules described by Nienow et al. (1977).

Mixing time was determined using a conductivity meter. The method of Kramers et al. (1953), with a pulse tracer input and measurement of the system response at two positions, i.e., one just below the surface and one at the vessel bottom, was followed. Some of these runs have been bench-marked using CFD.

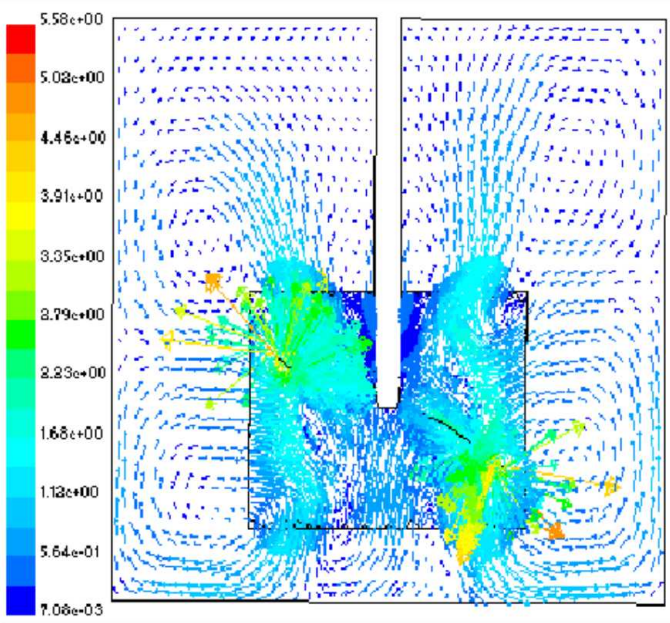

Figure 3. Liquid flow pattern of the NS impeller in turbulent flow in water at $N = 20$ s^{-1}, $T = 0.3$ m, $T/D = 3$. (Solution obtained by the sliding-mesh technique (Staykov et al., 2000).

The power was measured based on provisions for the specific impeller drives employed by drive producers, e.g., comprising a mixer controller and torque measuring device Servodyne (Cole Parmer). The electrical method was also applied.

Gas hold-up was measured by determining total liquid displacement and by conductometry (Nikov et al., 1991)

Results and Discussion

The following characteristics of the NS impeller were analyzed: flow pattern, mixing time, power and gas hold-up.

Flow Patterns

Visualization of Mixing Regimes by Dye-Tracers

The system response to a dye-tracer injection was studied. Visualization was achieved using nigrosine in a 0.3 m diameter vessel, as shown in Figure 2. The homogenization pattern and time of homogenization were captured and results obtained from Narcissus and a 45°-inclined blade turbine (IBT) (Masoud et al., 1999) were compared. In the figure, the flow differences identified at time 0 to 6, 12 and 16 s, were compared. It is seen that the IBT generates an axial flow forming one loop in the whole vessel, whereas the NS turbine draws the dye into an upper loop under the surface that at first is radial to the wall and then flows down to the impeller. Once the dye is distributed in the upper loop, it then disperses along the route of a loop under the impeller. In effect, the NS turbine forms two loops of axial flow that then transform into a radial near the impeller. Also, it is seen that the liquid discharge proceeds along the impeller shaft and then flows back toward the impeller periphery. As seen from the plan view through the vessel base, both impellers seem to exhibit a similar angular velocity. Based on this experiment, the Narcissus has been assigned an overall axial flow pattern with strong intermittent radial components.

Visualization of Mixing Flow Patterns by CFD Simulation

Detailed visualization analysis has been presented recently by Mavros et al. (2001). In this paper, only a velocity vector diagram obtained by the sliding mesh technique at 20 s^{-1} is presented (compare Figure 3). In the Figure, a well-defined axial up-flow starts at the impeller hub and a radial backflow entering the impeller periphery can be seen. Based on these results, the impeller could be described as a radial flow impeller with axial discharge. However, the phenomenon requires further consideration.

Flow Map

For gas dispersion, the type of diagram developed by Warmoeskerken and Smith (1989), has been generated. The plot is shown in Figure 4. The results are presented in terms of flow (Fl_G) and Froude (Fr) numbers; the experimental results are compared with the critical relationships for the flooding-loading (F) and complete dispersion (CD) regimes for a six flat-blade disc turbine:

$$Fl_F = 30\,Fr\left(\frac{T}{D}\right)^{-3.5} \tag{1}$$

and

$$Fl_{CD} = 13\,Fr^2\left(\frac{T}{D}\right)^{-5} \tag{2}$$

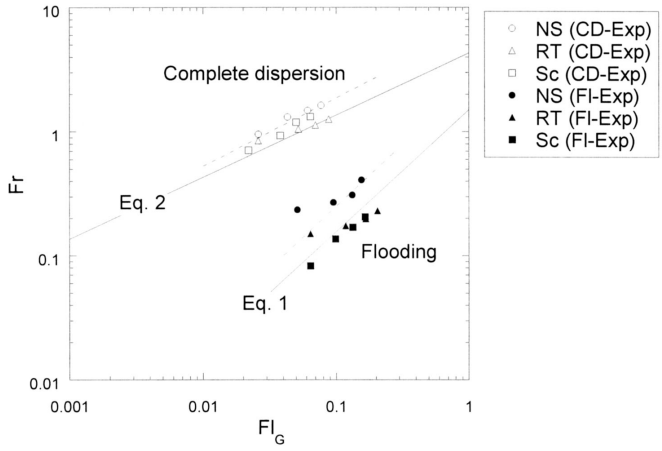

Figure 4. Flow regimes for the Narcissus impeller (NS) and the Rushton (RT) and Scaba (Sc) turbines registered in this study. The dotted lines illustrate the most probable critical boundaries obtained for the NS impeller. The solid lines refer to Equations (1) and (2) reported in the literature (Tatterson, 1991).

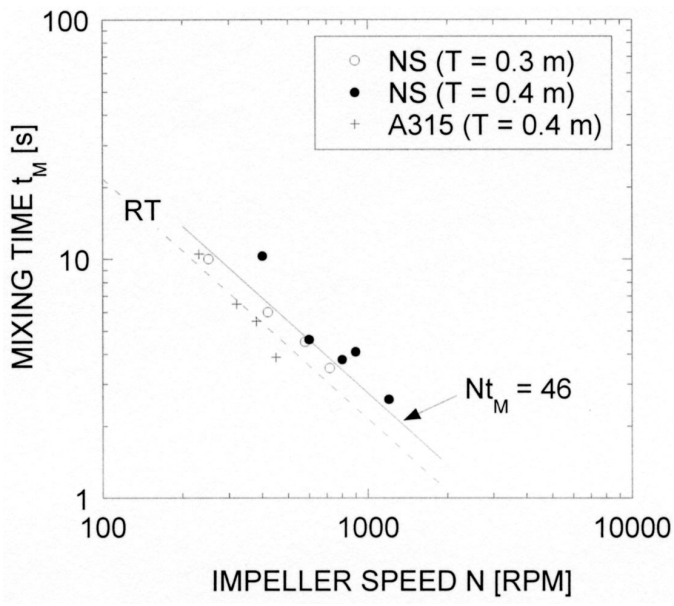

Figure 5. Experimental mixing time results for the NS impeller (T = 0.3 m and 0.4 m) and A315 (T = 0.4 m) obtained in this study, compared with a correlation developed for the Rushton turbine (the dotted line) by Moo-Young (see Tatterson, 1991). The course of line Nt_M = 46 is illustrated

It can be seen that the critical lines Fr versus Fl_G for the flooding-loading and for the complete dispersion regimes of the NS impeller are close to the lines reported for disc-style turbines (Tatterson, 1991). Yet one might observe that the NS would require a 20% larger diameter in order to avoid flooding and to handle as much gas as the stable, non-flooded hollow blades. Referring to the low power number of the Narcissus (Kraitschev et al, 1999), no significant loss of power would be required to maintain good gas dispersion or corresponding energy-savings. NS efficiency is illustrated further by the data for aeration power and gas hold-up.

Using the energy dissipation model, the gas handling ability at equal ε_T and D/T for different impellers can be compared. For example, using the disc-style turbine RT with $Fl_F = 0.1$ and $Fr = 0.15$ as the basis, $N_F = 3.2\ s^{-1}$, $\varepsilon_T = 0.11$ W/kg, and $(Q_G)_F = 0.7$ L/s are determined. For NS at $\varepsilon_T = 0.11$ W/kg, one obtains $N_F = 5.2\ s^{-1}$, $Fr = 0.36$, $Fl_F = 0.16$ and $(Q_G)_F = 1.8$ L/s. For Sc turbines at $\varepsilon_T = 0.11$ W/kg one obtains $N_F = 4.7\ s^{-1}$, $Fr = 0.27$, $Fl_F = 0.23$ and $(Q_G)_F = 1.9$ L/s. Consequently, the gas handling capacity of NS is comparable with Sc.

Mixing Time

Mixing time for the NS impeller was determined in ungassed conditions in two vessels, namely $T = 0.3$ m and $T = 0.4$ m. The results for NS and A315 obtained in the turbulent flow regime (i.e., for $Re > 10^4$) for the two vessel diameters are plotted in Figure 5. Reference results for Rushton turbines (RT) from Moo-Young et al. (1972) are illustrated by a dotted line.

As seen from the figure, in the turbulent flow regime the three impellers have similar performance showing dimensionless mixing time $Nt_M \approx$ 40-50 s, the differences being within the limits of experimental error. These results compare well with those reported for radial turbines (i.e. between 36 and 60 s), as seen also from the correlation in the figure (Tatterson, 1991).
Mixing time and circulation time were related by the equation:

$$t_C = \frac{t_M}{2} \qquad (3)$$

Applying the Van de Vusse model (Strenk, 1975) and considering t_c to be equal to the mean residence time in the overall flow loop,

$$t_C = \frac{V}{Q_L} \qquad (4)$$

where flow rate Q_l was calculated and the pumping capacity of the NS impeller $Fl_l \cong 0.85$ was determined. As seen from Figure 5 at equal N, the t_M of RT is 2 s lower. However, when comparing at equal rate of energy dissipation, ε_T = 1 W/kg for NS at 600 rpm and RT at 375 rpm, this difference declines to zero value.

Using the generalized correlation of Nienow (1996, 1997), mixing time at an energy dissipation rate of $\varepsilon_T \cong 1$ W/kg should be less than 7 s. On the basis of NS experimental results and from the difference between neighbouring peaks in conductivity variation at 1 W/kg, a typical mixing time of about 5 s was determined. A mixing time 6 s and a flow number 0.87 was obtained by CFD. This value compares favourably with that of 0.56 reported for fluid-foil impellers (Oldshue and Wheetman, 1988).

Power Requirements

Power at Ungassed Conditions

Figure 6a compares the NS power number for cylindrical vessels with power numbers of other impellers, e.g., the Scaba 6SRGT and the Lightnin A315 tested in this study under similar conditions. Two vessel and impeller sizes, namely T = 0.3 and 0.4 m with T/D = 3 were studied. A Rushton turbine reference line, as taken from the literature (Mezaki et al., 2000), is shown for comparison. Results indicate that Narcissus power numbers for the turbulent mixing regime were as low as 1.0 ± 0.2.

In view of testing the impeller for specific applications, e.g., the three-phase processing of mineral dispersions, a square

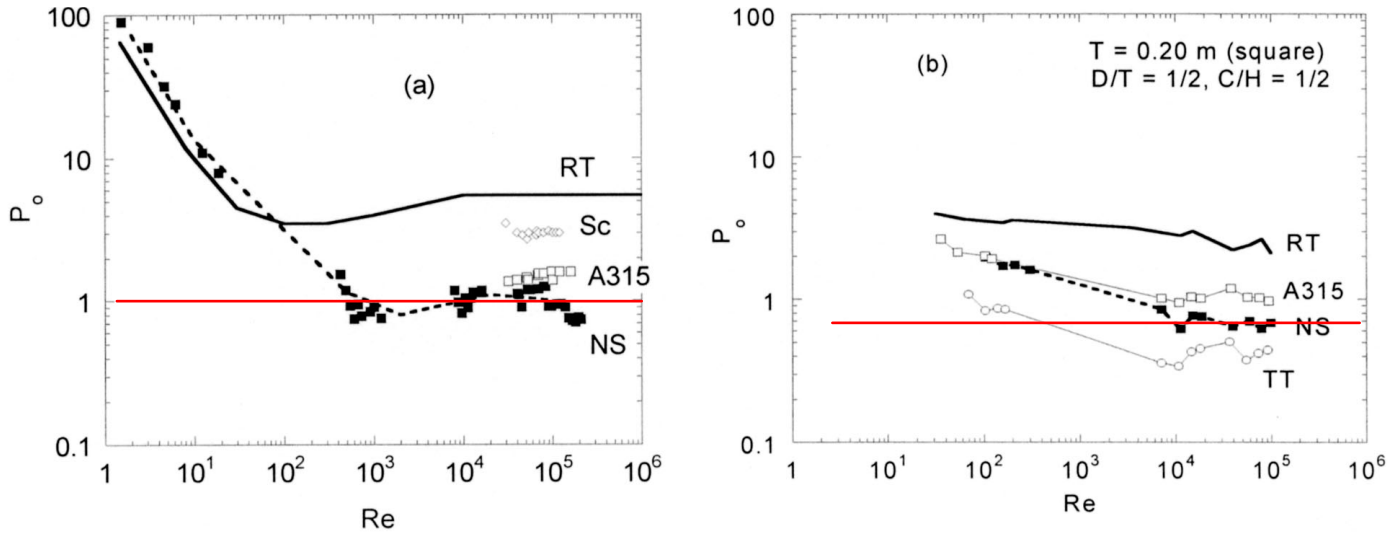

Figure 6. Power characteristic of the NS impeller, the Lightnin A315, the Mixel TT axial-flow agitators, the Rushton (RT) and Scaba (Sc) turbines in: (a) a cylindrical vessel and (b) in a square vessel. The solid lines of RT are taken from the literature, as follows: (a) Muzaki et al., 2000; and (b) Roustan and Pharmond (1988).

vessel was also studied. The power characteristics in the square tank are shown in Figure 6b, where the NS is compared to other agitators, namely the Mixel TT, the A315, and the Rushton turbines. The results for NS in the turbulent mixing regime show a *Po* as low as 0.9, which is similar to the value obtained in cylindrical vessels. The reference line (RT) in Figure 6b is from Roustan and Pharmond (1988).

Comparing the power and the discharge flow numbers and matching their ratio Po/Fl_L = 1.3 (after Nagata, 1975), one could classify Narcissus as a circulation flow impeller with moderate shear.

Aeration Power

The Narcissus impeller has a high solidity ratio, which should in principle result in a relatively high effectiveness in gassed fermentation media. Consequently, special attention has been paid to aeration power. The relationship of aeration power versus gas flow number Fl_G is shown in Figure 7. The experimental data correspond to Fr = 0.34 and Fr = 1.35. Parallel to NS power characteristics at N = 5 s^{-1} and N = 9 s^{-1}, aeration power has also been measured for Rushton turbines at the same rotation frequencies, and for Scaba (Sc) and A315 agitators at 10 s^{-1}. The energy dissipation rates corresponding to the above frequencies were 0.1 W/kg and 0.48 W/kg for NS, 0.46 W/kg and 2.7 W/kg for RT, and 0.7 W/kg and 0.4 W/kg for Sc and A315, respectively. Thus, the aeration power of the different impellers could be compared at ε_T ~ 0.4 W/kg. One can see that the power reduction on gassing for NS is weak and close to the one registered for A315 in this study. The power performance of NS and A315 at equal energy dissipation levels is comparable and improved with regard to the disc-style turbine. The A315 data obtained in the present study coincide with published data for this impeller (Baker and Van den Akker, 1994).

Gas Hold-up

The gas hold-up is related to the power per unit volume and to the impeller system. Figure 8 presents results obtained for relative gas flow rates of 1 vvm, and corresponding to the mid-range gas flow numbers registered in Figure 7. Two cases are considered: one with gas fed into water corresponding to the turbulent mixing regime, and another with gas fed into a 0.5% xanthan gum solution corresponding to turbulent transition.

In general, the gas hold-up found for NS was slightly higher than that generated by Rushton turbines. However, in some cases, as seen for the pseudo-plastic xanthan gum solution, the gas hold-up increased rapidly with power. This effect may be explained by the lower drag-reducing property of the NS blade shape in polymer solutions when compared to a flat blade impeller, and relates to pressure and drag distribution. Comparative mass transfer data obtained in xanthan gum solutions at an equal dissipation power of 0.8 W/kg showed the increase of K_La between NS and RT turbines as a ratio of 2:1 (Martinov and Vlaev, 2002).

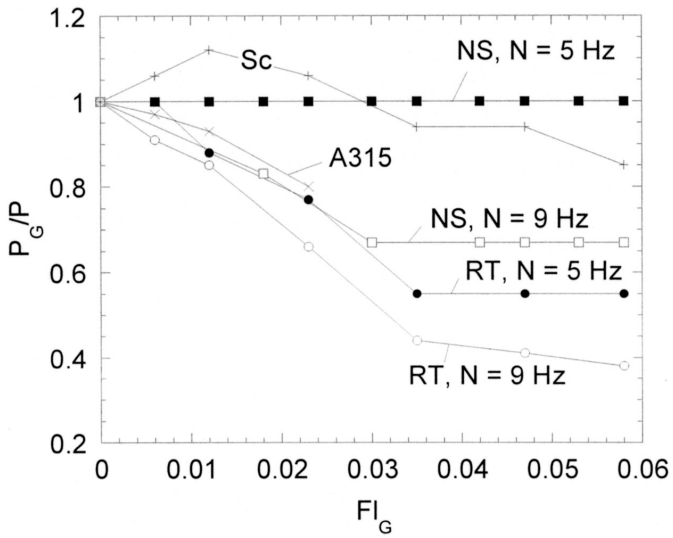

Figure 7. Gassed power ratio vs. aeration flow number of NS, RT and Sc and A315 turbines, as registered in this study.

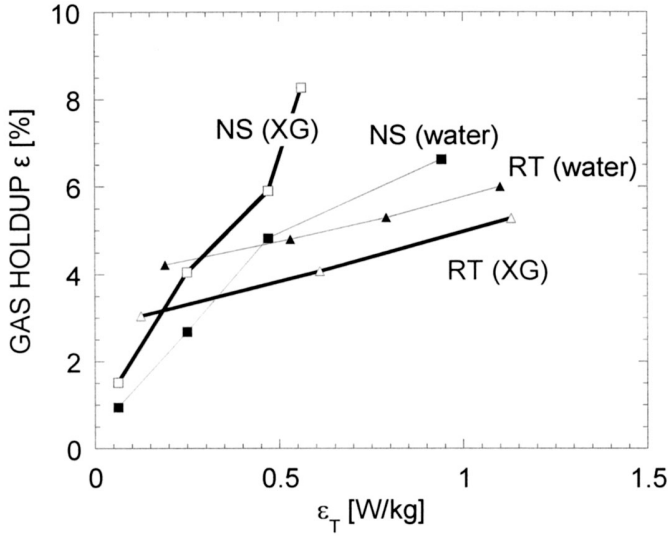

Figure 8. Gas hold-up in relation to the specific power consumption for the NS impeller and the Rushton turbine, for water and xanthan gum (XG) solution.

Conclusions

The operational characteristics of a new, energy-saving fluid foil impeller have been identified. The data confirm its high efficiency and validate a high gas hold-up generated at low input power. Compared to the many conventional disc-style turbines now employed in antibiotic production, the impeller shows improved aeration and blending characteristics. Its shape reduces its power number significantly, while its pumping capacity remains high. The loss of power on gassing is found to be moderate and the low power number suggests that an increase in its gas handling capacity would be obtained by increasing its size. The impeller exhibits a mixed axial and radial flow pattern that contrasts to the ones known for conventional turbines. In order to complete NS characterization, more information is needed for the impeller velocity contours, for its mass and heat transfer characteristics, as well for its performance in multiple configurations. Respecting the warning (Oldshue, 1989) and the experimental evidence (Mavros et al., 1996) that viscosity alters flow patterns in high-solidity ratio axial flow impellers, a CFD analysis of flow patterns at increased viscosities is envisaged in the future.

Acknowledgements

The authors gratefully acknowledge financial support from the Commission of the European Communities under INCO-COPERNICUS Contract No. IC15-CT98-0502.

Nomenclature

C	agitator clearance from vessel bottom, (m)
D	impeller diameter, (m)
Fl	flow number, (Q/ND^3)
Fr	Froude number, (N^2D/g)
K_La	volumetric mass transfer coefficient, (s^{-1})
N	impeller rotational speed, (rpm or s^{-1})
P	power, (W)
Po	power number, ($P/N^3D^5\rho$)
Q	volumetric flow rate, (m^3/s)
Re	Reynolds number, ($ND^2\rho/\mu$)
T	vessel diameter, (m)
t	time, (s)
t_M	mixing time, (s)
V	liquid volume, (m^3)

Greek Symbols

α	blade front edge angle to horizontal plane
ε	gas hold-up, (m^3/m^3)
ε_T	turbulent energy dissipation rate, (W/kg)
μ	viscosity, (Pa·s)
ρ	density, (kg/m^3)

Identifiers

C	circulation
CD	complete dispersion
F	flooding
G	gas
L	liquid

References

Baker, A. and H.E.A. van den Akker, "Gas–Liquid Contacting with Axial Flow Impellers", Trans. I. Chem. E. **72**A, 573–577 (1994).

Bertrand, J. and C. Xuereb, "Some Aspects of CFD on Mixing: Industrial Applications," in "Proc. 3rd Int. Symp. Mixing in Ind. Proc.", Osaka, Japan (1999), pp. 1–12.

Brucato, A., M. Ciafolo, F. Grisafi, and G. Micale, "Numerical Prediction of Flow Fields in Baffled Stirred Vessels: Comparison of Alternative Modeling Approaches", Chem. Eng. Sci. **53**, 3653–3684 (1998).

Chhabra, R.P. and J.F. Richardson, "Non-Newtonian Flow in the Process Industries", Butterworth-Heinemann, Oxford, UK (1999), pp. 337–340.

EKATO, "Process Improvement with a Novel Gassing Impeller", EKATO Mitteilung No. 18 (1998), pp. 1–8.

Fort, I., J. Medek and F. Ambros, "Power Input of Aerated Axial Flow Impellers", Chem. Biochem. Eng. Q. **13**(3), 127–132 (1999).

Jenne, M. and M. Reuss, "A Critical Assessment on the Use of k-ε Turbulence Models for Simulation of the Turbulent Liquid Flow Induced by a Rushton Turbine in Baffled Stirred-Tank Reactors", Chem. Eng. Sci. **54**, 3921–3941 (1999)

Kraitschev, S., V. Lossev, S.D. Vlaev and M. Valeva, "Energy-saving in Gas–Liquid Mixing Using the NS Impeller", Int. Chem. Eng. Symp. Ser. **146**, 245–252 (1999).

Kramers, H., G.M. Baars and W.H. Knoll, "A Comparative Study on the Rate of Mixing in Stirred Tanks", Chem. Eng. Sci. **2**, 35–42 (1953).

Lossev, V., S. Kraitschev, S.D. Vlaev and R. Mann, "Experience with a New Impeller", Paper presented at 16th NAMF Mixing Conference, Williamsburg, VA (1997).

Martinov, M. and S. D. Vlaev, "Average Shear Rate and Power Consumption of a Curved-Blade Impeller for Agitation of Shear-Thinning Fluids", Bulg. Chem. Commun. **31**, 471–476 (1999).

Martinov, M. and S.D. Vlaev, "Increasing Gas–Liquid Mass Transfer in Stirred Power Law Fluids by Using a New Energy-Saving Impeller, Chem. Biochem. Eng. Q. **16**, 1–6 (2002).

Masoud, R., P.R. Senior and R. Mann, "Image-Reconstruction 3-D Visual Modelling of Stirred Vessel Mixing for an Inclined-Blade Impeller", Int. Chem. Eng. Symp. Ser. **146**, 245–252 (1999).

Mavros P., C. Xuereb and J. Bertrand, "Determination of 3-D Flow Fields in Agitated Vessels by Laser-Doppler Velocimetry: Effect of Impeller Type and Liquid Viscosity on Liquid Flow Patterns", Chem. Eng. Res. Des. **74**A, 658–668 (1996).

Mavros, P., "Flow Visualization in Stirred Vessels: Part 1. Experimental Techniques", Chem. Eng. Res. Des. **79**A(2), 113–127 (2001).

Mavros, P., R. Mann, S.D. Vlaev and J. Bertrand, "Experimental Visualization and CFD Simulation of Flow Patterns Induced by a Novel Energy-Saving Dual-Configuration Impeller in Stirred Vessels", Trans. I. Chem. E. **79**A, 857–866 (2001).

Mezaki, R., M. Mochizuki, and K. Ogawa, "Engineering Data on Mixing", Elsevier Science B.V., Amsterdam (2000), pp. 119, 128, 220, 222.

Mishra, V.P., K.N. Dyster, Z. Jaworski, A. Nienow and J. McKemmie, "A Study of an Up- and a Down-pumping Wide Blade Hydrofoil Impeller: Part I. LDA Measurements", Can. J. Chem. Eng. ***76***, 577–588 (1998).

Moo-Young, M., K. Tichar and F.A.L. Dullien, "The Blending Efficiencies of Some Impellers in Batch Mixing, AIChE J. **18**, 178–182 (1972).

Nagata, S., "Mixing Principles and Applications", Wiley, New York, NY (1975), pp. 136–138.

Nienow, A.W., D.J. Wisdom and J.C. Middleton, "The Effect of Scale and Geometry of Flooding, Recirculation, and Power in Gassed Stirred Vessels", in "Proc. 2nd Europ. Conf. on Mixing", Cambridge, UK (1977), pp. F1/16.

Nienow, A., "Gas–Liquid Mixing Studies: Comparison of Rushton Turbines with Some ModernImpellers", Trans. Inst. Chem. Eng. **74**(A), 417–423 (1996).

Nienow, A.W., "On Impeller Circulation and Mixing Effectiveness in the Turbulent Flow Regime", Chem. Eng. Sci. **52**, 2557–2565 (1997).

Nikov, I., P.J. Carreau and C. Guy, "Axial Phase Distribution and Homogenisation in Three-phase Fluidized Beds", Chem. Eng. Comm. **104**, 153–165 (1991).

Oldshue, J.Y. and R.J. Wheetman, "Power, Flow and Shear Characteristics of Mixing Impellers", in "Proc. 6th Eur. Conf. on Mixing", Pavia, Italy (1988), p. 43.

Oldshue, J.Y., "Fluid Mixing in 1989", Chem. Eng. Prog. **85**, 33–42 (1989).

Pešl, L. and P. Seichter, "Evaluation of a Novel Energy-saving Impeller for Chemical Process Industries", in "Proc. 14th Int. Congress of Chem. and Process Engineering CHISA2000 CD-ROM", Paper P1.51, August, 27/31, Prague, Czech Republic (2000).

Roustan, M. and J.C. Pharmond, "Agitation et mélange", Techniques de i'Ingeniuer, Toulouse, France (1988), pp. A10, A5900.

Staykov, P., S.D. Vlaev and R. Popov, "Problems in CFD Simulation of a Novel Impeller with Fluid Foil Shape", in "Proc. 1st South-Eastern European Fluent Users Group Meeting", October 24th, Thessaloniki, Greece (2000), pp. S4–1 S4–8.

Strenk, F., "Mixing and Mixing Equipment" (in Russian), Khemia, Leningrad (1975), pp. 131–133.

Tatterson, G., "Fluid Mixing and Gas Dispersion in Agitated Tanks", McGraw-Hill, NY (1991), pp. 231, 437.

Vlaev, S.D. and M. Martinov, "Shape Effects on Impeller Power Characteristics for Mixing and Gassing Power Law Fluids", Inst. Chem. Eng. Symp. Ser. **146**, 253–262 (1999).

Vlaev, S.D., P. Staykov, R. Mann, H. Hristov and P. Mavros, "Experimental and CFD Characterization of a New Energy-saving Mixing Impeller for the Process Industries", Paper presented at 18th North American Mixing Conference, Pocono Manor, PA, June 24-29, (2001).

Warmoeskerken, M.M.C.G. and J.M. Smith, "The Hollow Blade Agitator for Dispersion and Mass Transfer", Chem. Eng. Res. Des. ***67***, 193–198 (1989).

Manuscript received October 17, 2001; revised manuscript received April 22, 2002; accepted for publication June 5, 2002.